RSC Advances




ROYAL SOCIETY OF CHEMISTRY

www.rsc.org/advances

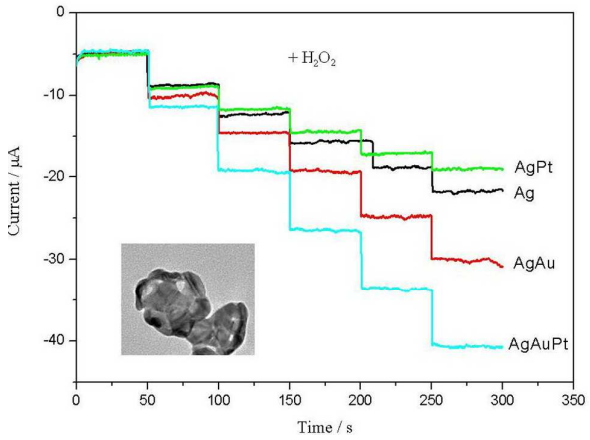


AgAuPt hybrid nanocages modified electrode showed high sensitivity for the detection of hydrogen peroxide.

Journal Name

RSCPublishing

ARTICLE

# AgAuPt nanocages for highly sensitive detection of hydrogen peroxide

Cite this: DOI: 10.1039/xoxxoooooox

Yang Peng, Ziren Yan, Ying Wu, and Junwei Di*,

Received ooth January 2014,
Accepted ooth January 2014

DOI: 10.1039/xoxxoooooox

www.rsc.org/

The electrocatalytical efficiency of metal nanoparticles depends on their structures as well as compositions. The analytic performance of four Ag-based metal (Ag, AgPt, AgAu, and AgAuPt) nanostructures modified electrode for detection of hydrogen peroxide was investigated. Silver nanoparticles (Ag NPs) were deposited on indium tin oxide (ITO) film coated glass surface. Then Ag NPs were used as sacrificed template to generate AgPt, AgAu, and AgAuPt hybrid hollow nanostructures using galvanic replacement reaction. The AgAuPt nanocages (AgAuPt NCs) show the highest sensitivity for electrochemical detection of hydrogen peroxide in all metal nanostructures. This modified electrode exhibits a linear current response to hydrogen peroxide concentration in the range of 4 μM – 4 mM with detection limit of 2 μM at applied potential of -0.35V. These results indicate that AgAuPt NCs could be a promising electrochemical material for detection of hydrogen peroxide.

## 1. Introduction

Hydrogen peroxide ($H_2O_2$) determination has been increasing interest due to its great importance in biology, food, pharmaceutical, clinical, textile, and environment applications.[1-3] $H_2O_2$ is also a product of some enzymatic reactions, such as glucose oxidase,[4] cholesterol oxidase,[5] lactate oxidase,[6] and urate oxidase.[7] Therefore, it is practically important to develop a reliable, sensitive, rapid and low-cost method for determination of $H_2O_2$.

Because of intrinsic simplicity, high sensitivity and good selectivity, electrochemical methods have been extensively used in detection of $H_2O_2$.[1,2] Recently, numerous electrochemical $H_2O_2$ sensors, based on enzyme[8-10] and non-enzyme working electrodes,[11-13] has been fabricated. Nevertheless, the relatively high cost and the instability limit the application of enzyme-based biosensors. Therefore, it has attracted great attention for development of nonenzymatic sensors for sensitive determination of $H_2O_2$.

Nowadays, nanomaterials, especially the noble metal nanoparticles, are widely used to develop enzyme-free electrochemical sensors due to their high catalytic activity for $H_2O_2$. Noble metal nanoparticles, such as silver nanoparticles (Ag NPs),[14-16] gold nanoparticles (Au NPs),[17] and platinum nanoparticles (Pt NPs),[18,19] have been developed as electrocatalysts to detect trace $H_2O_2$. Among these nanoparticles, Ag NPs exhibit high electrocatalytic activity for $H_2O_2$ detection.[20-22] On the other hand, metallic alloy nanoparticles maybe show the favorable catalytic properties over monometallic counterparts and unique advantages from nanostructures. Several different dimetallic nanomaterials have been used as amperometric sensor for determination of $H_2O_2$.[23-25]

The catalytic efficiency (the response current) is generally related to the electrode surface area. Hollow nanostructures of noble metals have high specific surface area and easy permeability, which can enhance reactivity. Moreover, hollow metallic nanomaterials exhibit high catalytic activities different from their solid counterparts with the advantages of low density and reduction of material. For examples, gold nanocages (Au NCs),[26] nanoporous gold [27] and platinum hollow nanospheres [28] have been used to fabricate non-enzyme sensor for detection of $H_2O_2$.

With the advent of new synthetic strategy and surface science modeling facilities, it has become possible to design and construct nanostructures with desired properties. For example, gavalnic replacement reaction provides a straightforward and versatile route to metallic nanostructures with hollow nanocrystals and controllable elemental composition.[29] In this work, Ag NPs were deposited on indium tin oxide (ITO) film coated glass surface and then as sacrificed template to prepare AgPt, AgAu, and AgAuPt hybrid hollow nanostructures using galvanic replacement. The electrochemical catalytic activity of the as-prepared metals modified ITO electrodes in response to $H_2O_2$ was investigated. The AgAuPt nanocages (AgAuPt NCs) based sensor exhibited the highest sensitivity for the determination of $H_2O_2$. Herein, it is demonstrated that the high sensitivity is benefit from both hollow nanostructures and synergistic effect of metals.

## 2. Experimental

### 2.1. Materials

Silver nitrate ($AgNO_3$), hydrogen tetrachloroaurate ($HAuCl_4$), potassium tetrachloroplatinate ($K_2PtCl_4$), hydrogen peroxide ($H_2O_2$), disodium hydrogen phosphate ($Na_2HPO_4$), sodium dihydrogen phosphate ($NaH_2PO_4$), and potassium nitrate ($KNO_3$) were purchased from Sinopharm Chemical Reagent Co. Ltd. (Shanghai, China). Phosphate buffer solution (PBS, pH 7.0) was prepared with $Na_2HPO_4$ and $NaH_2PO_4$. All reagents were of analytical grade and used as received without further treatment. High-quality deionized water (resistivity >18.0 MΩ cm) used for experiments was prepared by a water purification system (Milli-Q, Millipore).

### 2.2. Apparatus

All electrochemical experiments were performed with a RST 5200 electrochemical workstation (Suzhou Risetest Instrument Co., Ltd., China). A conventional three electrode system was used in this experiment. The bare or modified ITO electrode was used the working electrode. A Pt wire was used as the counter electrode and a saturated calomel electrode (SCE) was used as reference electrode. Scanning electron microscope (SEM) images were taken on an S-4700 field-emission scanning electron microscopy (Hitachi, Japan). Transmission electron microscope (TEM) image was carried out on a FEI Tecnai G2 20 transmission electron microscope. The sample was prepared by dropping the mixed solution on a copper grid and allowing the solvent to evaporate. X-ray diffraction (XRD) pattern was obtained by X'Pert-Pro MPD (Panalytical, Holland). UV-visible absorption spectra were recorded by UV-3600 UV–VIS–NIR spectrophotometer (Shimadzu, Japan) against a bare ITO slide as the reference.

### 2.3. Preparation of metal nanostructures modified electrodes

The divided ITO glass strip (50mm × 5 mm) was cleaned using dilute $NH_3 \cdot H_2O$, ethanol, and water for 10 min sequentially in an ultrasonic bath. The Ag NPs were synthesized by square wave cyclic voltammetric method. The electrolyte consisted of 0.2 mM $AgNO_3$ and 0.1 M $KNO_3$ and kept at 30 °C. The Ag NPs were electrodeposited at potential of -0.6 V for 3 s and then grown in the range of -0.3 ~ 0 V for 40 cycles with frequency 10 Hz, amplitude 25 mV and potential step 2 mV. Next, AgAuPt NCs were prepared by galvanic replacement reaction. The ITO-based Ag NPs were incubated in 0.15 mM $HAuCl_4$ and 0.05 mM $K_2PtCl_4$ for 2 h at 50 °C. The concentration of metal precursors used is discussed in section 3.3. Finally, the AgAuPt NCs modified electrode was rinsed with water and dried in nitrogen atmosphere. For comparison, the AgAu and AgPt hybrid nanomaterials modified electrodes were fabricated by the same procedure only containing 0.2 mM $HAuCl_4$ and $K_2PtCl_4$, respectively.

## 3. Result and discussion

### 3.1. Characterization of metal nanostructures

Ag, AgPt, AgAu, and AgAuPt nanostructures were prepared for the comparison of the $H_2O_2$ biosensor properties depending on composition of metal nanostructures. Figure 1 shows the UV-visible absorption spectra of the prepared metal nanomaterials. The localized surface plasmon resonance (LSPR) peak of Ag NPs deposited on transparent ITO substrate was located at ~450 nm. The galvanic replacement reaction between Ag atoms and Pt ions is similar to that of between Ag atoms and Au ions. After reacting with $K_2PtCl_4$ solution, the LSPR peak of Ag NPs became small. This suggested that most of Ag was replaced with Pt and formed hollow nanostructures. When Ag NPs were incubated in $HAuCl_4$ solution for 2 h, a new peak appeared at ~1030 nm. It was attributed to the formation of silver-gold nanocages (AgAu NCs). As replacement solution was mixture of $HAuCl_4$ and $K_2PtCl_4$, the obtained LSPR band was similar to that of Au NCs but low its peak intensity, indicating the formation of AgAuPt nanocages (AgAuPt NCs).

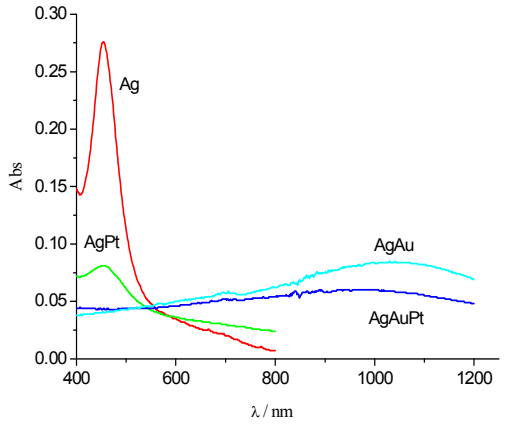


Fig. 1 UV-visible absorption spectra of silver nanoparticles deposited on ITO substrate and as sacrificed temple to generate AgPt, AgAu, AgAuPt hybrid nanostructures using galvanic replacement reaction.

Figure 2 shows the SEM images of prepared metal nanostructures on ITO substrate surface. SEM images of Ag NPs showed non-agglomerated uniformly distributing on ITO substrate surface (Figure 2A). These particles are of half-spherical nature with average size of ~80 nm. After replacement reaction with $K_2PtCl_4$, the particles showed small pores and became some agglomerate (Figure 2B). Figure 2C displays the SEM images of AgAu NCs, where the pores in particles could be seen clearly. Figure 2D exhibits the SEM images of AgAuPt NCs. The morphologies of AgAuPt NCs were similar to that of Ag NPs and the size of pores in AgAuPt NCs was smaller than that of AgAu NCs. The partially different morphologies of the hybrid nanostructures may be attributed to different replacement ratio of Pt/Ag (2:1), whereas for Au/Ag is 3:1.[30]

In order to get surface information about the metal nanostructures on ITO substrate, cyclic voltammogram of AgAuPt NCs was recorded in 0.05 M $H_2SO_4$ in the potential range from -0.2 to 1.5 V. Three couple redox peaks of 0.37/0.13 V, 0.92/0.45 V, and 1.34/0.85 V corresponded to the redox of Ag, Pt, and Au, respectively. The charge associated with reduction of metal oxide species of the electrode surface can be used to estimate the ratio of

Pt/Au in particle composition.[31] The Pt/Au ratio in AgAuPt NCs was calculated to be approximately 2%, which was much lower than that of 25% in electrolyte. This is because that the rate of replacement reaction between the platinum ions and silver atoms in Ag NP template is slower than that between gold ions and silver atoms.[30]

In order to further characterize the structures of metal nanoparticles, the AgAuPt NCs were released from ITO substrate into ethanol solution upon sonication. Figure 3B shows the TEM image of AgAuPt NCs peeled off from ITO surface. It is clearly observed that hollow structures were formed. This further demonstrates the formation of AgAuPt nanocages.

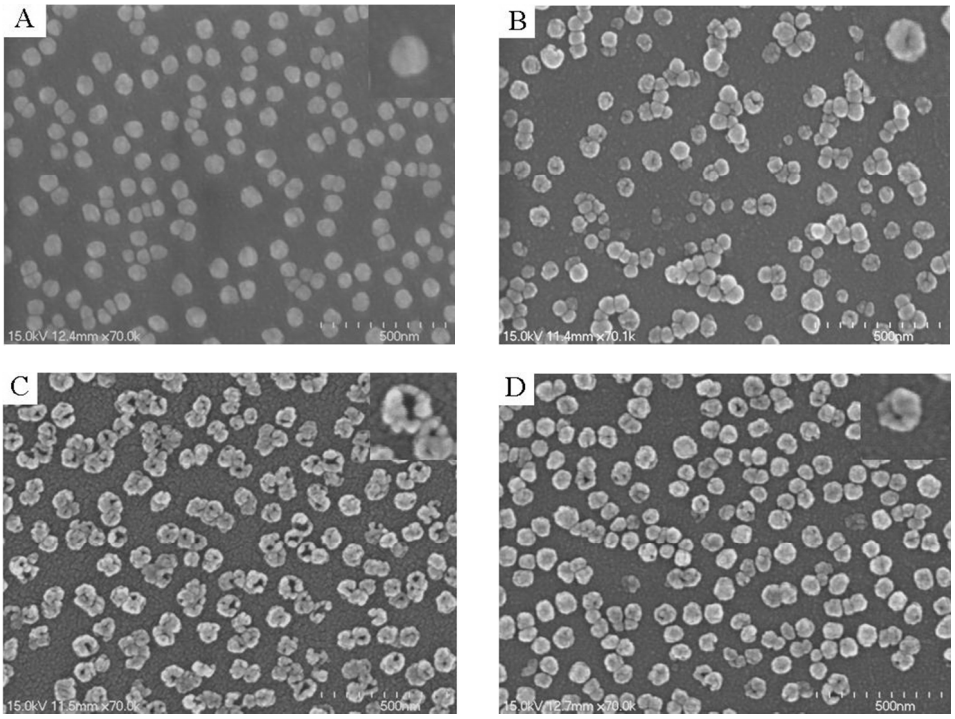


Fig. 2 SEM images of Ag (A), AgPt (B), AgAu (C), and AgAuPt nanostructures (D). Inset: its high resolution image.

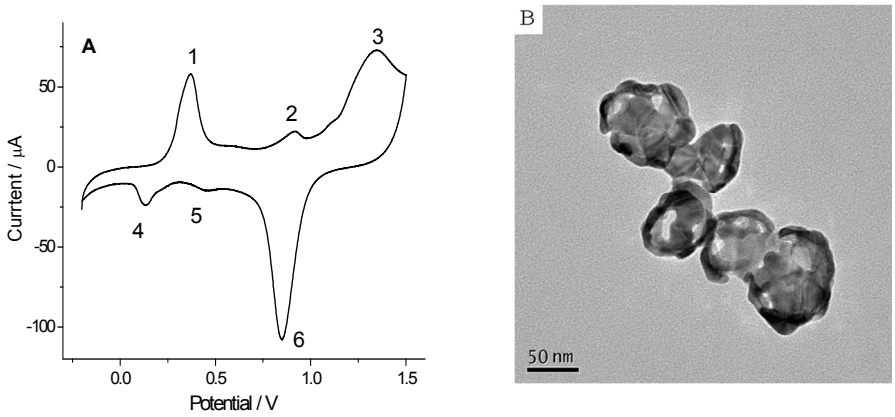


Fig. 3 Cyclic voltammogram of the AgAuPt NCs grown on ITO substrate in 0.5M $H_2SO_4$ at potential scan rate of 50 mV/s (A), and TEM image of AgAuPt NCs peeled from ITO substrate.

Journal Name RSCPublishing

ARTICLE

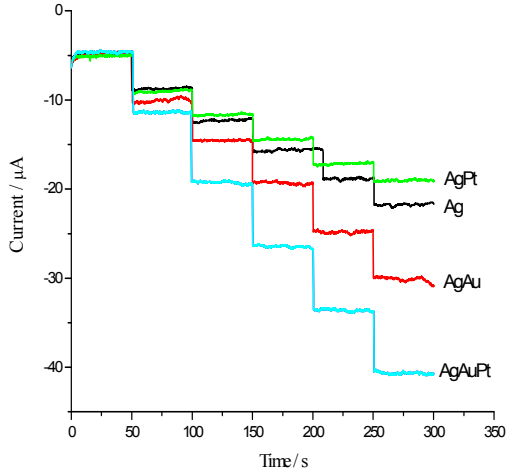


Fig. 4 Amperometric response of metal nanostructures modified electrode with successive additions of 0.1 mM $H_2O_2$ in 0.05 M phosphate buffer solution at applied potential of -0.35 V.

### 3.2. Voltammetric behavior of the modified electrodes to $H_2O_2$

According to the previous reports,[32,33] $H_2O_2$ can be decomposed in to $H_2O$ and $O_2$ under silver as catalyst in the solution of pH 7.0 phosphate buffer solution. Then the generated oxygen is reduced on the modified electrode. It can be used to detection of $H_2O_2$. Therefore, the mechanism for $H_2O_2$ reduction reactions at Ag-based modified electrode is shown below:

$$2H_2O_2 \xrightarrow{Ag} O_2 + 2H_2O \quad (1)$$

$$O_2 + 2e^- + 2H^+ \xrightarrow{\text{electrode}} H_2O_2 \quad (2)$$

Figure 4 shows the biosensor properties at different metallic nanostructures modified electrodes with successive addition of 0.1 mM $H_2O_2$. The amperometric response with Ag, AgPt, AgAu, and AgAuPt nanostructures showed current response of 3.1, 2.8, 5.2 and 7.2 μA, respectively. The current response for AgPt nanostructures was slight lower than that of Ag NPs. The result is some surprised because Pt is generally considered as good catalyst. This low response may be attributed to a few small pores of AgPt nanostructrures. However, the current response for AgAu NCs was markedly higher than that of Ag NPs. Moreover, the biosensor based on AgAuPt NCs exhibited a highest sensitivity in all modified electrodes. This is attributed to the porous structures and synergistic effect of AgAuPt hybrid metals. Therefore, AgAuPt NCs modified ITO electrode was employed in the next experiments for determination of $H_2O_2$. On the other hand, according to a recent study by Bard et al.,[34] Pt counter electrode may dissolve into electrolyte in acidic media, which influences the reaction on working electrode. In our work, the synthesis of metal nanomaterials and measurements of $H_2O_2$ were carried out in neutral media. Moreover, the amperometric responses of $H_2O_2$ at various metal structures were stable, demonstrating this effect could be negligible.

### 3.3. Effect of composition and applied potentials

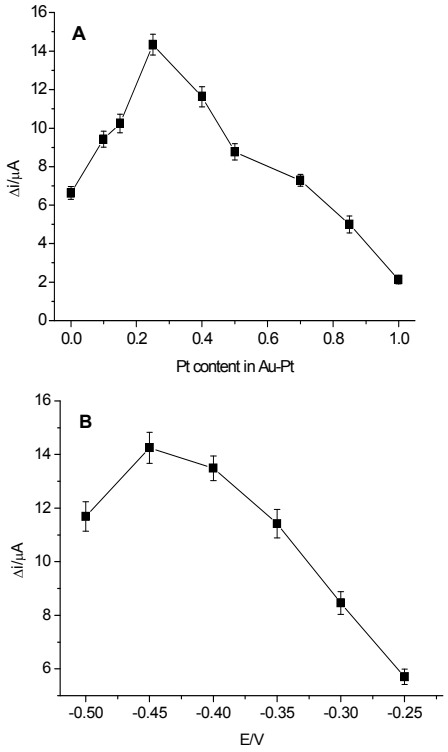


Fig. 5 Amperometric response of the AgAuPt NCs modified electrodes with various Pt content in total 0.2 mM Au-Pt electrolyte to 0.2 mM $H_2O_2$ (A), and .at different applied potentials (B).

Figure 5A shows the electrode properties are affected by the Pt content in total concentration of 0.2 mM Au-Pt electrolyte. The amperometric responses were monitored at the optimum conditions when 0.2 mM $H_2O_2$ was injected into 0.05 M phosphate buffer solution. The current increased first with increasing Pt content from 0 to 25% in total 0.2 mM Au-Pt electrolyte and then decreased with further increase Pt content. The current response showed the maximum value at 25% content Pt in Au-Pt electrolyte. Please note that Pt content in AgAuPt NCs was much lower according to the above result.

Figure 5B displays the effect of applied potentials on the reduction of $H_2O_2$ at the AgAuPt NCs modified electrode. The reduction currents increased with decreasing the applied potentials from -0.25 V to -0.45 V and then decreased with further decrease of

applied potentials. Although the largest response was observed at a potential of -0.45 V, the large background current was also obtained. For this reason, we chose the applied potential of -0.35 V for amperometric measurement of $H_2O_2$ concentration in all experiments.

### 3.4. Analytical performance of the sensor to $H_2O_2$

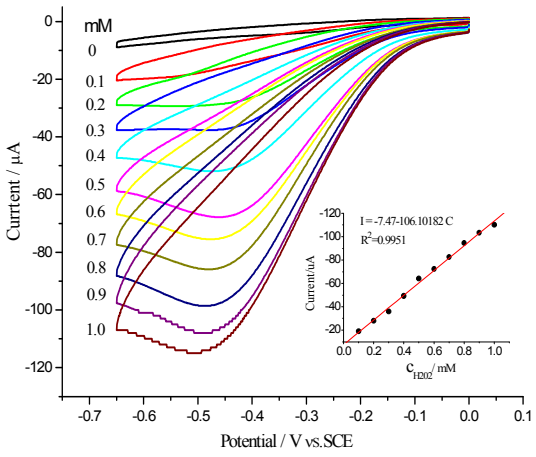


Fig. 6 cyclic voltammetric measurements of various concentrations of $H_2O_2$ in 0.05 M phosphate buffer solution at AgAuPt NCs modified electrode. Inset: calibration curve. Scan rate of 100 mV/s.

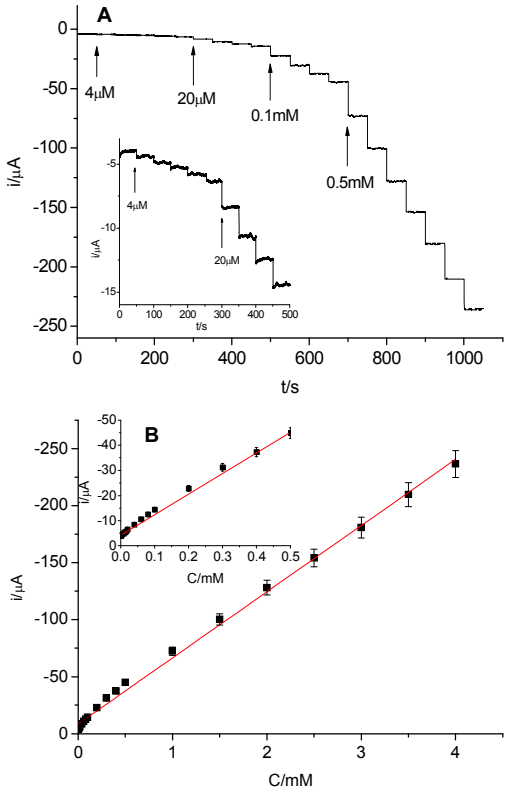


Fig. 7 An amperometric response of the AgAuPt NCs modified electrode with successive addition of $H_2O_2$ to 0.05 M phosphate buffer solution at the applied potential of -0.35 V (A) and its corresponding calibration plot (B).

The hybrid metal nanomaterials modified electrode should be confirmed for its practicality to determination of $H_2O_2$. Under optimum conditions, various concentrations of $H_2O_2$ were first measured using cyclic voltammograms. The cyclic voltammetric responses of various concentration of $H_2O_2$ in phosphate buffer solution (pH 7.0) were recorded at the AgAuPt NCs modified ITO electrode (Figure 6). The cathodic peak currents were direct proportional to the concentrations of $H_2O_2$.

Figure 7 illustrates a typical current-time curve of the AgAuPt NCs modified electrode after continuous injections of $H_2O_2$ concentration to the phosphate buffer solution. The time required to reach 95% of the maximum steady-state current was less 1 s, indicating a fast amperometric response behavior. With the increasing $H_2O_2$ concentration, the amperometric response increased linearly in the range from 4 μM to 4 mM with a correlation coefficient of 0.9971 and a slope of 56.7 μA $mM^{-1}$ (sensitivity). The detection limit was estimated to be 2 μM at a signal-to-noise ratio of 3. Table 1 shows a comparison between this electrode with some metal nanostructures modified electrodes for electrochemical detection of $H_2O_2$.

Table 1 Comparison of the performance of various modified electrodes for $H_2O_2$ detection.

| electrodes | Linear range | Detection limit/μM | Ref. |
|---|---|---|---|
| Graphene-Ag NPs | 100 μM – 41 mM | 35 | 16 |
| Graphene-Au NRs | 30 μM – 5 mM | 10 | 17 |
| PtCu NCs | 5 μM – 22.25 mM | 5 | 23 |
| Au-Pt NPs/TiOx NT | 10 – 80 μM | 10 | 24 |
| Nanoporous gold | 10 μM – 8 mM | 3.26 | 27 |
| AgAuPt NCs/ITO | 4 μM – 4 mM | 2 | This work |

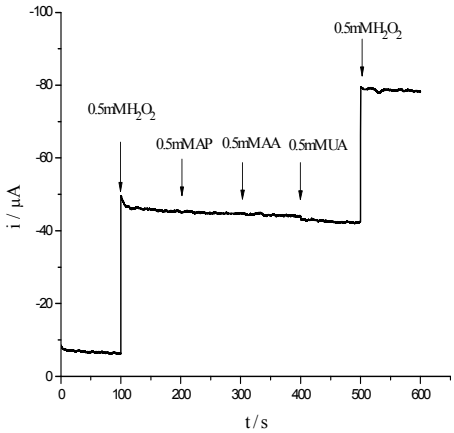


Fig. 8 Amperometric response of AgAuPt NCs modified ITO electrode to 0.5 mM $H_2O_2$ and different interferences 0.5 mM 4-acetamidophenol (AP), 0.5 mM ascorbic acid (AA), 0.5 mM uric acid (UA) in nitrogen saturated 0.05 M phosphate buffer solution at the applied potential of -0.35 V.

Selectivity is an important factor for the performance of a sensor. As shown in Figure 8, amperometric response of 0.5 mM $H_2O_2$ at AgAuPt NCs modified ITO electrode was monitored at applied potential of -0.35 V in the presence of electrochemical interfering species including 4-acetamidophenol (AP), ascorbic acid (AA), and uric acid (UA) in the concentration level of 0.5 mM each. AgAuPt NCs modified ITO electrode showed excellent selectivity as inferred from the stable response for the reduction of $H_2O_2$. It can be observed that the tested interferences could not significantly interfere with the detection of $H_2O_2$.

The fabrication reproducibility was also evaluated from the response to 0.1 mM $H_2O_2$ at five different AgAuPt NCs modified ITO electrodes fabricated simultaneously in the same conditions, and an acceptable relative standard deviation (RSD) of 4.3% was obtained. The stabilization action of the AgAuPt NCs modified ITO electrode was investigated after being stored in dry conditions at room temperature for 40 days and measured at intervals over 3-4 days. The current response to $H_2O_2$ remained about 91% compared to that of initial current.

The determination of $H_2O_2$ in cosmetic was performed on the modified electrode utilizing standard addition method. The cosmetic sample was obtained from local supermarket. After the amperometric response was determined in 5.0 mL of 0.05 M phosphate buffer solution (pH 7.0) containing sample 0.5 mL, which depended on the concentration of $H_2O_2$, four 10 μL of 0.01 M $H_2O_2$ solutions were successively added to the system for measurements. The $H_2O_2$ level was determined to be 0.143±0.005 mM (n=3). The recoveries for the assay were between 95.8% – 109.7% for detections.

## 4. Conclusion

From the comparison of the analytical performance of the four Ag-based nanostructures modified electrodes, it is demonstrated that AgAuPt NCs show highest sensitivity for the detection of $H_2O_2$. The developed AgAuPt NCs modified ITO electrode shows excellent electrocatalytic activity for detection of $H_2O_2$ due to the unique catalytic properties of metals, high surface area of nanostructures and synergistic effect of hybrid metals. This electrode exhibits a wide linear range, low detection limit, good reproducibility and stability. The proposed method is thus expected to develop new opportunities for fabrication of reliable sensor devices for measuring $H_2O_2$ concentration in chemical, clinical, food, beverage, and environmental analyses fields.

## Acknowledgements

This work was financially supported by the National Natural Science Foundation of China (No. 21075086, 21475092), Natural Science Foundation of Jiangsu Province (BK2011273), the Project of Scientific and Technologic Infrastructure of Suzhou (SZS201207) and the Priority Academic Program Development of Jiangsu Higher Education Institutions.

### Notes and references

The Key Lab of Health Chemistry and Molecular Diagnosis of Suzhou, College of Chemistry, Chemical Engineering and Material Science, Soochow University, Suzhou, 215123, PR China

1 W. Chen, S. Cai, Q. Ren, W. Wen and Y. Zhao, *Analyst*, 2012, **137**, 49.
2 S. Chen, R. Yuan, Y. Chai and F. Hu, *Microchim. Acta,* 2013, **180**,15.
3 L. Campanella, R. Roversi, M.P. Sammartino and M. Tomassetti, *J. Pharmaceut. Biomed.*1998, **18,** 105.
4. A. S. Campbell, C. Dong, J. S. Dordick, C. Z. Dinu, *Process Biochem.* 2013, **48**, 1355.
5. Md. M. Rahman, X. Li , J. Kim, B. O. Lim, A. J. S. Ahammad, J. Lee, *Sens. Actuators, B: Chem.* 2014, 202, 536.
6. M. Gamero, M. Sosna, F. Pariente, E. Lorenzo, P.N. Bartlett, C. Alonso, *Talanta* 2012, 94, 328.
7. E. Akyilmaz, M. K. Sezgintürk, E. Dinçkaya, *Talanta* 2003, 61, 73.
8 J. Wan, J. Bi, P. Du and S. Zhang, *Anal. Biochem.,* 2009, **386**, 256.
9 B. Wang, J. Zhang, G. Cheng and S. Dong, *Anal. Chim. Acta,* 2000, **407**, 111.
10 L. Gao and Q. Gao, *Biosens. Bioelectron.,* 2007, **22**, 1454.
11 S. Ghaderi and M. A. Mehrgardi, *Bioelectrochemistry,* 2014, **98** , 64.
12 S. Wu, H. Zhao, H. Ju, C. Shi and J. Zhao, *Electrochem. Commun.,* 2006, **8**, 1197.
13 C. Hsu, K. Chang and J. Kuo, *Food Control,* 2008, **19**, 223.
14 X. C. Song, X. Wang, Y. F. Zheng, R. Ma and H. Y. Yin, *J. Nanopart. Res.,* 2011, **13**, 5449.
15 J. Yin, X. Qi, L. Yang, G. Hao, J. Li and J. Zhong, *Electrochim. Acta*, 2011, **56**, 3884.
16 X. Liu, X. Xu, H. Zhu and X. Yang, *Anal. Methods*, 2013, **5**, 2298.
17 P. Pang, Z. Yang, S. Xiao, J. Xie, Y. Zhang and Y. Gao, *J. Electroanal. Chem.*, 2014, **727**, 27.
18 S. Chakraborty and C. R. Raj, *Biosens.Bioelectron.*, 2009, **24**, 3264.
19 F. Xu, Y. Sun, Y. Zhang, Y. Shi, Z. Wen and Z. Li, *Electrochem. Commun.*, 2011, **13**, 1131.
20 A. Safavi, N. Maleki and E. Farjami, *Electroanalysis*, 2009, **21**, 1533 .
21 Y. Ding, G. Jin and J. Yin, *Chinese J. Chem.*, 2007, **25**, 1094.
22 B. L. Li, J. R. Chen, H. Q. Luo and N. B. Li, *J. Electroanal. Chem.*, 2013, **706**, 64.
23 L. Tian, X. Zhong, W. Hu, B. Liu and Y. Li, *Nanoscale Res. Lett*., 2014, **9**, 68 .
24 Q. Kang, L. Yang and Q. Cai, *Bioelectrochemistry*, 2008, **74**, 62.
25 K. Chen, K. C. Pillai, J. Rick, C. Pan, S. Wang, C. Liu and B. Hwang, *Biosens. Bioelectron.*, 2012, **33**, 120.
26 Y. Zhang, Y. Sun, Z. Liu, F. Xu, K. Cui, Y. Shi, Z. Wen and Z. Li, *J. Electroanal. Chem*., 2011, **656**, 23.
27 F. Meng, X. Yan, J. Liu, J. Gu and Z. Zou, *Electrochim. Acta*, 2011, **56**, 4657.



 

28 J. Li, R. Yuan, Y. Chai, T. Zhang and X. Che, *Microchim. Acta*, 2010, **171**, 125.
29 C. M. Cobley and Y. Xia, *Mat. Sci. Eng. R*, 2010, **70**, 44.
30 M. A. Mahmoud and M. A. El-Sayed, *Langmuir,* 2012, **28**, 4051.
31 A. Habrioux, E. Sibert, K. Servat, W. Vogel, K. B. Kokoh and N. Alonso-Vante, *J. Phys. Chem. B,* 2007, **111***,* 10329.
32 X. Li, Y. Liu, L. Zheng, M. Dong, Z. Xue, X. Lu and X. Liu, *Electrochim. Acta,* 2013, **113**, 170.
33 W. Zhao, H. Wang, X. Qin, X. Wang, Z. Zhao, Z. Miao, L. Chen, M. Shan, Y. Fang and Q. Chen, *Talanta*, 2009, **80**, 1029.
34 C. Gu, B. C. Norris, F. F. Fan, C. W. Bielawski, A. J. Bard, *ACS Catal.* 2012, **2**, 746.